DESIGN OF NEW COATINGS AND SINTERED MATERIALS BASED ON MIXED RARE EARTH OXIDES

RADU ROBERT PITICESCU [1)], MIRCEA CORBAN [1)], MARIA LUISA GRILLI [2)], FELIX BALIMA [3)] and MYTHILI PRAKASAM [3)]

[1)] National R&D Institute for Nonferrous and Rare Metals-IMNR, Romania
[2)] ENEA Cassacia Research Center, Rome, Italy
[3)] CNRS-Institute for Chemistry of Condensed Materials, Bordeaux, France
e-mail: rpiticescu@imnr.ro

Abstract

Monazite is one of the most valuable natural resources of rare earth elements used in high added value applications in many areas, including catalysis, glassmaking, metallurgy, optoelectronics, batteries and coatings for extreme environments. Extraction of individual lanthanides requires very complex and reagents consuming sequential processes due to their very similar electronic configuration and physical-chemical properties. The complexity of the separation process is reflected in the high price of the individual lanthanides.
The aim of the paper is to demonstrate the potential use of mixed rare earth oxides obtained directly from monazite concentrates with naturally occurring composition, as dopant in the design of high temperature oxide coatings and sintered materials. Some results toward two potential applications are presented: coatings architectures based on mixed REOs-doped zirconia obtained by combinatorial electron beam physical vapour deposition process with high temperature resistance properties and sintered materials for solid oxide fuel cells with controlled ionic conductivity.

Keywords: *Rare earth oxides, Zirconia, EB-PVD coatings, SOFC*

Introduction

Rare Earth Oxides (REOs) are materials already used in mature markets (catalysts, glassmaking, metallurgy), having a large increasing trend in newer, high-tech markets (batteries, ceramics and permanent magnets) [1]. Typical abundance for RE elements are in the range from 1.1 (Tb) to 68 ppm (Ce). Their actual availability relates to their specific mineralogy and mining of poor ores is leading to processing of large amounts of ore, increasing the environmental footprint [2].Monazite with the generic formula (Ce, La, Nd, Th, Y, Dy, Sm)(PO_4) is one of the most valuable natural resources of rare earth elements. Concentration and separation of RE requires very complex processes, including flotation, gravity or magnetic separation to produce concentrates that are further leached with inorganic acids or alkaline aqueous solutions. Further separation stages by successive solvent extraction followed by precipitation using (NH_4)HCO_3 or oxalic acid ($C_2H_2O_4$) lead to precipitates that are heated to form individual REOs [3].

Recently considerable interest has been paid to the design and preparation of RE oxide nanomaterials due to their great potential applications closely related to their size, chemical composition and morphology [4]. $La(OH)_3$, $Nd(OH)_3$, $Pr(OH)_3$, $Sm(OH)_3$, $Gd(OH)_3$, and $Er(OH)_3$ with rod-like morphology were fabricated via a hydrothermal approach [5, 6]. It was shown that REOs may avoid grain size coarsening due to interface segregation in doped zirconia ceramics enhancing its thermo-mechanical properties. The absolute grain boundary energy of Gd-doped nanocrystalline ZrO_2 vs. grain size can reach a quasi-zero energy state (0.05 J/m2), when a critical dopant enrichment is achieved, until a temperature threshold where the dopant re-dissolves in the crystalline bulk [7]. Co-doping ofZrO_2 ceramics with different ratios of Y_2O_3 and CeO_2 was also used to obtain sintered ceramics with improved sinterability [8]. The co-doping of zirconia with different REOs was also reported to improve the thermal properties of thermal barrier coatings [9].In addition, small additions of e.g. Y, Zr, Ce, Ti and Hf improves the alloys oxidation properties by balancing the outward diffusion of metal ions and the inward diffusion of oxygen, which leads to a balanced oxide growth and thus a reduction of mechanical stresses and/or porosity in the oxide layer [10].

Combinations of oxygen vacancies and RE ions leading to the long-ranged hysteresis and improved ionic conductivity was studied in the co-doped sintered $((Y_{0.75}La_{0.25})_{1-x}Gd_x)_{0.18}Zr_{0.82}O_{2-\delta}$ system [10]. The energy values x-dependencies (x=0…1) for the bulk and grain boundary conductions are strongly related to the ionic radii of the trivalent REs ions because the states of oxygen vacancies, which are substantially responsible for ionic conductions may capture the vacancies at lower temperatures.

Modelling the ionic conductivity in bulk nanostructured doped ZrO_2 was proposed [11] and a crystalline size of yttria-doped zirconia around 20 nm was calculated as critical to reduce activation energy by a grain boundary ionic conductivity mechanism.

These previous results lead us to the idea to obtain directly from monazite collective REOs and study their behaviour as dopants to improve thermal properties of thermal barrier coatings and ionic conductivity of zirconia ceramics.

Experimental set-up

The precursor solution was prepared by dissolution of pure $ZrCl_4$ into distilled water, filtering to eliminate insoluble particles and dissolving rare earth oxides in the appropriate amount under vigorous stirring. The pH of the solution was adjusted to the desired value by mixing it with ammonium hydroxide solution. REOs-doped zirconia powders were then obtained by hydrothermal treatment of the suspension in a 5 l Teflon autoclave (Berghoff, Germany) for 2 h in the temperature range 150–250 ^{0}C. The precipitates were filtered, washed with distilled water to remove the soluble chlorides and ethanol to reduce agglomeration and dried for several hours in air at 110 ^{0}C.

Multiple thin films with controlled thickness were deposited by physical vapour deposition in high vacuum (10^{-6}…10^{-7} bar) on stainless steel and NIMONIC superalloys using a custom-designed combinatorial Electron Beam-PVD system from Torr Inc. USA, presented in Fig.1.

The EB-PVD system is endowed with 4 independent e-guns, each of them having a carrousel of 4 crucibles around, allowing to deposit up to 16 components (Fig. 1.a). The maximum size of the top substrate rotating parallel to the bottom plate (Fig. 1.b) reaches 350x350 mm and may be heated with the help of a UV-lamp system up to 800^{0}C (Fig. 1.c). Continuous remove of coated substrates and feeding new clean substrates is possible via a lock vacuum chamber (Fig.1.d). A second rotating support perpendicular to the central axis is also mounted to allow coating both faces of a rectangular substrate with maximum sizes 350x350mm (Fig. 1.e).

Heating is done periodically with the help of a chamber containing UV-lamps (Fig. 1.f). The thickness of coated material is continuously monitored with the help of a quartz balance. The process is computer controlled, the software allows following and adjusting the power of each of the 4 EB guns, vacuum inside the chamber, heating temperature and deposition rate.

Sintered materials with the same composition were obtained by spark plasma sintering (SPS) Model SPS-511S / SPS-515S 2500 °C - 5T, applying simultaneous temperature and pressure up to 1000 MPa within a controlled atmosphere.

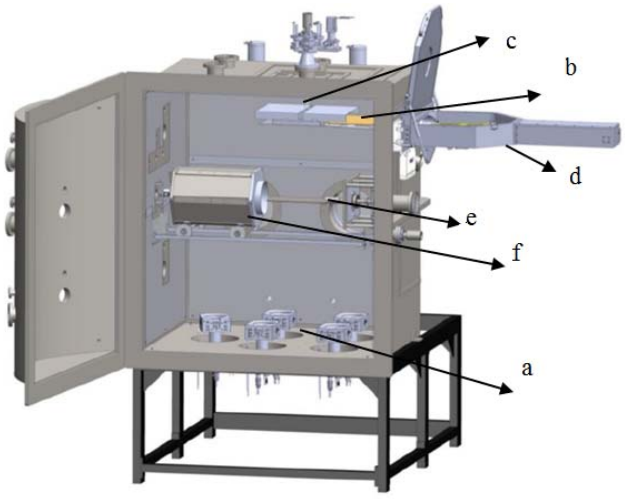


Fig. 1. Schematic presentation of multiple EB-PVD coating system

Chemical composition of powders was analysed by Inductive Coupled Plasma Optical Spectrometer (ICP-OES Agilent 725). Phase composition of powders was performed on a Bruker D8 Advanced Diffractometer, which uses the Bragg-Brentano method, Copper Kα radiation and SOL X detector in order to remove Copper Kβ radiation. Data acquisition and processing was performed with the software DIFFRAC^{PLUS} Bruker AXS package Release 2006 and ICDD database, Powder Diffraction File, edited by International Centre for Diffraction Data 2006. The obtained data content from XRD diffraction patterns concern information about nature and phase quantities present in samples, crystal structure, lattice parameters, crystallite's size and amorphous content. The mean crystallite sizes were calculated according to the Sherrer formula from the broadening of the [111] characteristic peak of the crystalline phases.

The morphology of spray dried aggregated nanopowders was analysed with a FEI 250 SEM system endowed with EDAX for chemical analysis of surfaces.

The tribology tests on un-coated and coated surfaces were performed using the universal CETR UMT-3 Bruker tribometer according to ASTM G77-98.

Thermal diffusivity measurements were carried out using a standard laser flash analyzer (LFA 457 Micro Flash). The effective ionic conductivity was measured using impedancemetry measurements set-up from ICMCB Bordeaux. Theoretical density of the powder was calculated with the formula below:

$$\rho = \frac{n \times A}{V_c \times N_A} \quad (1)$$

where: n - number of atoms associated with each unit cell; A- atomic weight (= 161.3 g/mol); n-coordination number =4; V_c - volume of the unit cell; N_A- Avogadro's number (6.022×10^{23} atoms/mol) and a is the lattice parameter.

The calculated theoretical density for REOs doped-ZrO_2 powder is 7.94g/cm^3. This value was used both in the calibration of quartz balance to monitor the coating thickness and for calculation of sintering degree.

Results and discussion

The hydrothermal synthesis parameters were estimated based on the thermodynamic modelling using the HSC Chemistry 9.0 software (Outotec, Finland), using E-pH (Pourbaix) diagrams considering all ionic and condensed species for the system Zr-La-O-H vs. solution pH for a maximum hydrothermal temperature 250^{0}C. Fig. 2 presents the diagrams obtained; it shows that formation of mixed oxide at 250 ^{0}C is expected to be optimized in the pH range 8-11.

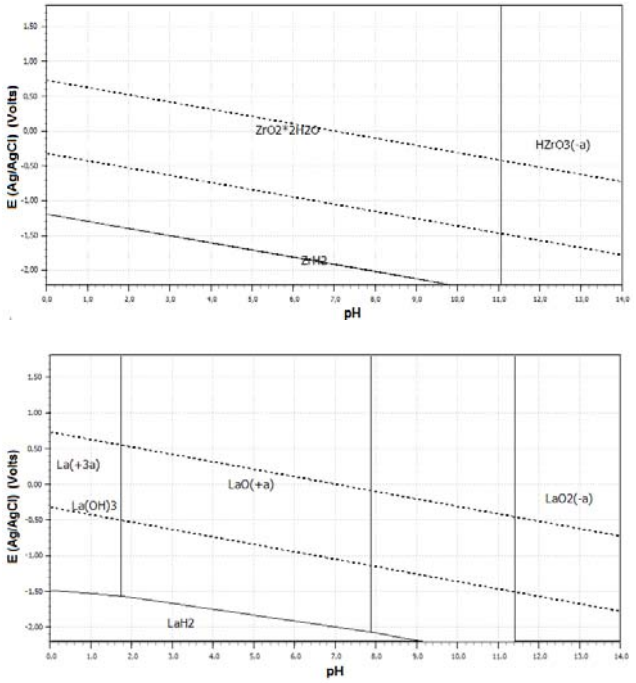


Fig. 2. Calculated E-pH diagrams for the system Zr-La-O-H at 250 ^{0}C

Table 1 presents the typical chemical composition and XRD analysis of one batch of REOs-doped ZrO_2 powder obtained by hydrothermal method. The ratio between the total content of REOs to ZrO_2 was calculated to correspond to 8 mol %.

Table 1. Chemical and phase composition of REOs-doped ZrO_2 powders

Sample code	**Chemical composition [wt %]**	**Phase composition**
ZrO_2-REO1	Zr=52.19 Y=0.46 La=3.49 Gd=0.278 Nd=2.33 Sm=0.409 Yb=0.0032	Centered-faced cubic major phase Lattice parameter a =3.589 Tetragonal minor phase Lattice parameters: a = 3.59840; b=3.59840; c=5.15200

Fig. 3 presents the XRD diagram of the sample compared to the standard 8 mol% Y_2O_3-ZrO_2 commercial powders (TOSOH).

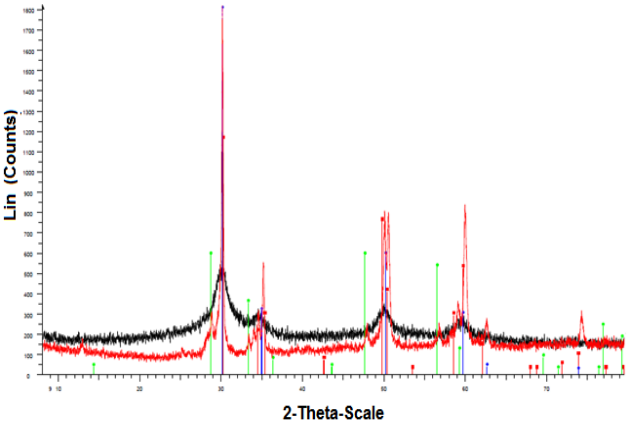


Fig. 3. XRD Diagram of ZrO_2-REO 1 sample (black) compared to standard cubic 8 mol% Y_2O_3-ZrO_2

Micrometrics powders with uniform grain sizes distribution showing well shaped prismatic faces are formed, as seen in the SEM picture from Fig. 4.

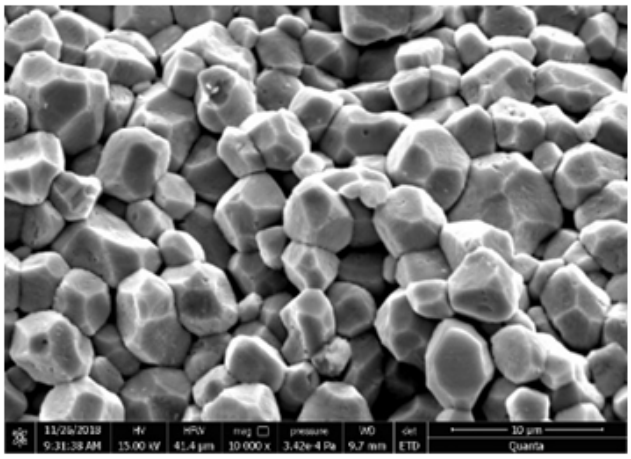


Fig. 4. SEM picture of ZrO_2-REO 1 sample

Different coatings architectures were obtained on stainless steel, Ni superalloys and graphite: REOs-doped ZrO_2; NiCrYAl/REOs-doped ZrO_2; NiCrYAl/REOs-doped ZrO_2/ZrB_2 and NiCrYAl/REOs-doped ZrO_2/ZrO_2/$La_2Zr_2O_7$. The coatings parameters for EB-PVD system were: deposition time - 360 min; work pressure in steady regime - 10^{-6} torr; steady state e-gun voltage - 10kV; e-gun current intensity - 260 mA: substrate temperature - 600 ^{0}C.

SEM pictures from Fig. 5 present the surface morphology of the coating NiCrYAl/REOs-doped ZrO_2/ZrB_2 on NIMONIC 80 alloy and the coating architecture in transversal section, respectively. Fig 6 presents the morphology and coating architecture of the same coating on high dense graphite substrates.

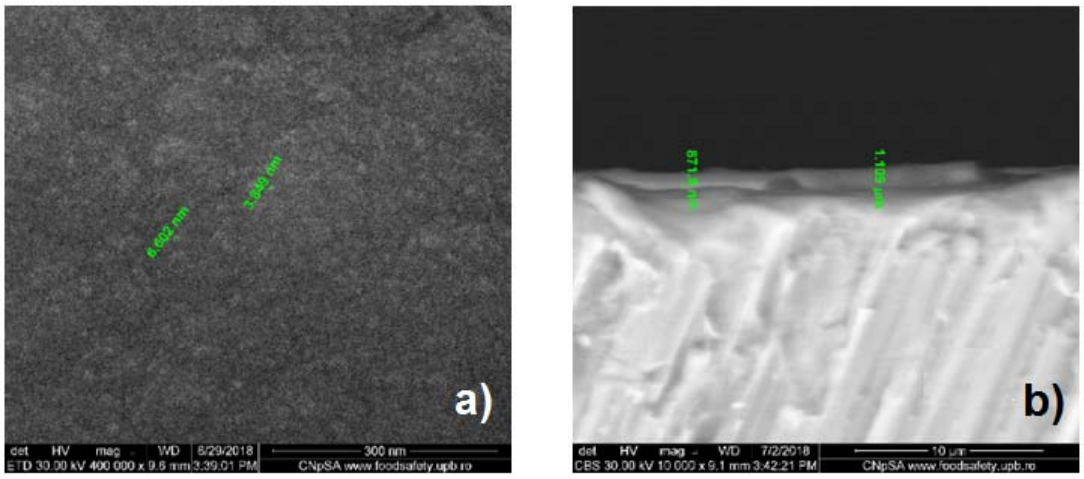


Fig. 5. SEM picture of NiCrYAl/REOs-doped ZrO_2/ZrB_2 coatings on NIMONIC 80:
a) surface morphology; b) cross section

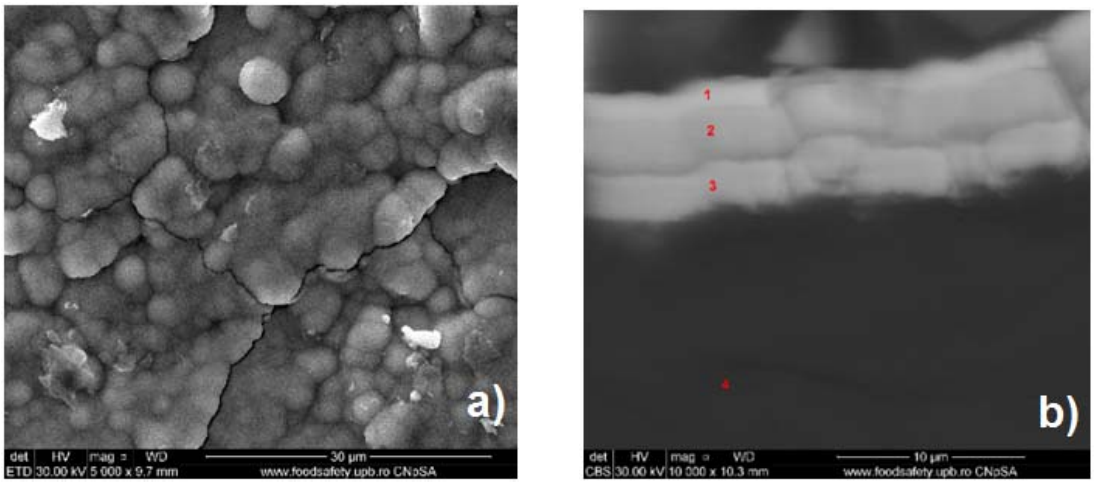


Fig. 6. SEM picture of NiCrYAl/REOs-doped ZrO_2/ZrB_2 coatings on graphite:
a) surface morphology; b) cross section

The coating obtained by EB-PVD on metallic substrate (NIMONIC 80 superalloy) consist of continuous and uniform REOs-doped zirconia layer with typical columnar growth and thickness around ~ 5 µm and the external protective ultra-high temperature ZrB_2 layer with thickness around ~ 1 µm and smooth surface morphology formed by dense-packed nanometric crystals.

The coating obtained by EB-PVD on dense graphite substrates are less uniform and their morphology is strongly influenced by the graphite topography, leading to larger crystals sizes and formation of some cracks and holes on the external layer coating.

The tribology analysis and the evolution of the friction coefficients with time are presented in Fig. 7. It may be observed the increase of the friction coefficient of the coated substrates, proving also the good coating adherence to the metallic substrate.

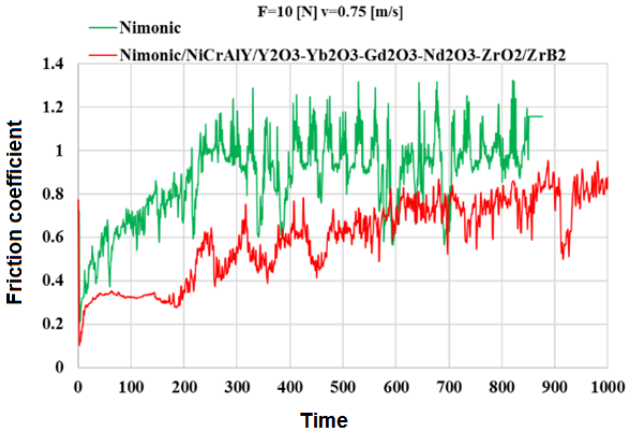


Fig. 7. Friction coefficients of un-coated NIMONIC 80substrate and NIMONIC 80 coated with NiCrYAl/ REOs-doped ZrO_2/ZrB_2 layers

The thermal diffusivity and impedance curves of sintered REOs-doped zirconia sintered materials compared to standard cubic 8 mol% Y_2O_3-doped ZrO_2 (both > 99% theoretical density obtained by SPS) are shown in Fig. 8.

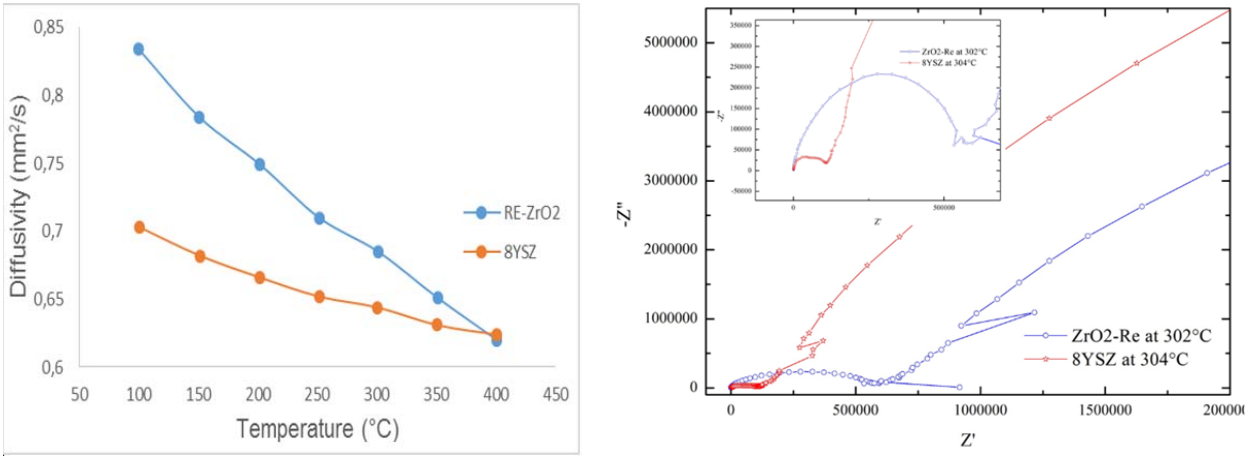


Fig. 8. Thermal diffusivity (left) and Nyquist impedance curves (right) of SPS sintered REOs-doped zirconia materials compared to standard cubic 8 mol% Y_2O_3-doped ZrO_2

The results prove that using mixed REOs as dopant increase the thermal conductivity and reduce the activation energy for the ionic conductivity in the range of 0.584 – 0.889 eV for REOs-doped ZrO_2 compared to 0.718 – 0.907 eV for 8 YSZ standard. First trials demonstrated that zirconia doped with mixed ROEs have a better ionic conductivity at moderated temperatures

Conclusions and future prospects

Zirconia nanopowders doped with mixed rare earth oxides have been successfully synthesized by a hydrothermal process and the powders have been used to obtain different coatings architectures by EB-PVD process and sintered pellets with densities >99% of the theoretical value by spark plasma sintering.

Coatings obtained by EB-PVD on NIMONIC 80 superalloy consisting of continuous and uniform REOs-doped zirconia layer with typical columnar growth and thickness around ~ 5 µm and an external protective ultra-high temperature ZrB_2 layer with thickness around ~ 1 µm having smooth surface morphology formed by dense-packed nanometric crystals and good friction properties and adherence were obtained. When dense graphite plates was used as substrates, layers with less uniform thickness, larger crystals sizes and formation of some cracks and holes on the external layer were obtained.

The measurement of thermal diffusivity and ionic conductivity of zirconia sintered materials doped with mixed REOs show that the activation energy of ionic conduction is reduced, having a high potential impact on future possible applications in SOFCs with moderate working temperature.

The works continue to refine the coatings architectures and adherence aiming to improve their functional properties for applications in thermal barrier coatings and corrosion protection in molten metal for nuclear energy applications. The sintering tests will be also continued to improve the ionic conductivity for better and cheaper SOFCs.

Acknowledgments

Research financed in the frame of ERAMIN II-COFUND programme, grant ID 87, contract UEFISCDI 50/01.04.2018 and Program Nucleu PN 19 19 04 01 financed by Romanian Ministry for Scientific Research and Innovation.

Special thanks to Dr. Vasile Bogdan from National Centre for Micro and Nanomaterials of the Politehnica University Bucharest for performing SEM analysis and Dr. Mihai Botan from INCAS Bucharest for tribology tests on coatings.

References

[1] Charalampide. G., Vatalis, K.I., Apostoplos, B., Nikolas, B.P. (2015) ″Rare Earth Elements: Industrial Applications and Economic Dependency of Europe″, Int. Conf. on Applied Economics (ICOAE), Kazan, Russia, Procedia Economics and Finance, Vol. 24, pp. 126-135.
[2] Haque, N., Hugues, A., Lim, S., Vernon, C. (2014) ″Rare Earth Elements: Overview of Mining, Mineralogy, Uses, Sustainability and Environmental Impact″, Resources, Vol. 3(4), pp. 614-635.
[3] Xie, F., Zhang, T.A., Dreisinger, D., Doyle, F. (2014) ″A critical review on solvent extraction of rare earths from aqueous solutions″, Minerals Engineering, Vol. 56, pp. 10-28.
[4] Yan, Z.-G., Yan, C.-H. (2008) ″Controlled synthesis of rare earth nanostructures″, Journal of Materials Chemistry, Vol. 18(42), pp. 5046–5059.
[5] Gschneider, K.A., Bunzli, J., Pecharski, V.C. editors (2011) ″Handbook on the Physics and Chemistry of Rare Earths″, Vol. 41, Elsevier,
[6] Li, C., Liu, H., Yang, J. (2015) ″A facile hydrothermal approach to the synthesis of nanoscale rare earth hydroxides″, Nanoscale Res. Letters, Vol. 10, 144.
[7] Nafsin, N., Castro, R.H.R. (2017) ″Direct measurement of quasi-zero grain boundary energies in ceramics″, Journal of Materials Research, Vol. 32(1), pp. 166-173.

[8] Dragut, D.V., Badilita, V., Motoc, A.M., Piticescu, R.R., Zhao, J., Hijji, H., Conte, L. (2017) ″Thermal stability and field assisted sintering of cerium-doped YSZ ceramic nanoparticles obtained via a hydrothermal process″, Manufacturing Review, Vol. 4, 11.

[9] Sobetkii, A., Rinaldi, A., Cuesta-Lopez, S., Prakasam, M., Largeteau, A., Plaiasu, G., Piticescu, R.R. (2017) ″Novel high temperature oxide ceramics coatings: synthesis, properties and applications″, Proceed. of Int. Conf. Frontiers in Materials Processing Applications, Research and Technology FiMPART, Bordeaux, France.

[10] Ekström, M., Thibblin, A., Tjernberg, A., Blomqvist, C., Jonsson, S. (2015) ″Evaluation of internal thermal barrier coatings for exhaust manifolds″, Surface and Coatings Technology, Vol. 272, pp. 198-212.

[11] Komine, S., Iimure, T., Iguchi, E. (2005) ″Co-doping effects on crystal structure and electric conduction in $((Y_{0.75}La_{0.25})_{1-x}Gd_x)_{0.18}Zr_{0.82}O_{2-\delta}$″, Solid State Ionics, Vol. 176(35-36), 2535-2543.

[12] Piticescu, R.R., Monty, C., Millers, D. (2005) ″Hydrothermal synthesis of nanostructured zirconia materials: Present state and future prospects″, Sensors and Actuators B: Chemicals, Vol. 109(1), pp. 102-106